

# **Assessing Psychological Stress During Physiological and Cognitive Tasks Using fNIRS**

Kailey Wheeler

Department of Biology, Thompson Rivers University

BIOL 4480: Directed Studies in Biology

Dr. Mark Rakobowchuk

April 23rd, 2025

## Abstract

**Background:** Memory retrieval tasks are commonly used to assess cognitive decline associated with aging, but anxiety can impair performance. Traditional questionnaire-based assessments of state anxiety may lack temporal precision. Objective physiological measurements capturing sympathetic activation (SA) offer a more reliable approach. This study explores the feasibility of using functional near-infrared spectroscopy (fNIRS) to simultaneously measure brain activity and stress through entropy values derived from pulsatile changes in the signal.

**Methods:** Fifteen healthy young adults completed two physical (cold pressor test, isometric handgrip) and two cognitive (unsolvable anagram, color–shape interference) stress tasks while fNIRS, blood pressure, and heart rate were monitored. Entropy-based metrics— Average Sample Entropy and Total Sample Entropy— were extracted from both fNIRS and arterial blood pressure signals during pre-task and during-task periods.

**Results:** fNIRS entropy (AvgSampEn and TotalSampEn) significantly increased from pre- to during-task across all four tasks ( $p = 0.023$ ,  $p = 0.036$ ), with no task  $\times$  time interaction. Mean arterial pressure increased significantly during all four tasks ( $p = 0.005$ ). Blood pressure entropy metrics varied by task.

**Conclusion:** These findings support the use of fNIRS-based entropy as a non-invasive measure of SA during both physical and cognitive stress. Uniform increases in fNIRS entropy suggest generalized sympathetic effects on cerebral perfusion, while peripheral responses varied by task. Future research should explore temporal dynamics and incorporate direct sympathetic measurements.

**Keywords:** functional near infrared spectroscopy, state anxiety, stress, working memory, sympathetic activity, entropy, brain imaging, age-related cognitive decline.

## Introduction

Memory retrieval tasks are commonly used in clinical settings to assess cognitive decline associated with aging (Salthouse, 2012). These tasks rely on an individual's ability to recall information, which can be adversely affected by state anxiety (Moran, 2016). Anxiety occurs when a person cannot generate a distinct pattern of action to eliminate or change the event that is perceived as a threat. State anxiety (current level of anxiety) is established by the level of test or trait anxiety (personality characteristic) and by situational stress (Eysenck et al., 2007; Naveh-Benjamin et al., 1981). Anxiety can impair working memory by disrupting attentional control, making it more difficult to focus on task-relevant information and ignore distractions. This interference is especially pronounced when anxiety-related thoughts consume cognitive resources needed for processing and temporarily storing information. The interpretations of the outcome of these memory retrieval tasks may be inaccurate if participants were experiencing acute anxiety at the time (Eysenck et al., 2007).

To ensure the validity of these cognitive assessments, it is important to measure the participant's state-anxiety. Although questionnaires are frequently used for this purpose, their reliability in capturing state anxiety is debatable, and their consistency can vary across repeated measures. Previous studies have shown that participants with highly variable anxiety scores across sessions did not show corresponding fluctuations in cognitive performance, suggesting that questionnaire-based assessments may fail to reflect true momentary emotional states of which impact cognitive functioning (Meissel & Salthouse, 2016). As such, employing physiological measures to assess state anxiety may offer a more reliable approach to correct for this potentially confounding factor.

Both elevated anxiety and acute stress have been shown to activate the sympathetic branch of the autonomic nervous system (Bigalke et al., 2023; Kim et al., 2025; Richards and Bertram, 2000). Sympathetic activation (SA) on target effectors causes measurable physiological responses such as heart rate, blood pressure, skin blood flow, sweat secretion, pupil dilation, etc (Macefield, 2021). Measuring these physiological responses to SA provides an indirect measurement of acute stress or anxiety. Recently, photoplethysmography (PPG) has been developed as a measurement of SA, by detecting changes in local blood oxygenation at the wrist or in the fingers. Recent research by Udhayakumar et al, 2023, has shown that this method could identify the onset of physiological stressors (e.g. the cold pressor test) by using infrared light to track fluctuations in blood flow with each heartbeat. They focused specifically on the pulsatile amplitude (AC component) of the PPG signal, which reflects beat-to-beat changes in peripheral blood volume, providing a direct indicator of vasomotor activity modulated by SA. To quantify the irregularity of these pulse amplitude fluctuations during stress, they extracted the nonlinear measures Average Sample Entropy (AvgSampEn) and Total Sample Entropy (TotalSampEn). The results showed that SA induced by the cold pressor and hand-grip tests led to significant changes in both AvgSampEn and TotalSampEn. Specifically, AvgSampEn increased during the initial stress response and decreased during recovery, and TotalSampEn varied minute-by-minute.

A brain-imaging device commonly used to assess age-related cognitive decline is functional near-infrared spectroscopy (fNIRS) (Udina et al., 2019). fNIRS utilizes infrared light to measure brain activity by detecting changes in oxygenated and deoxygenated hemoglobin in the brain and scalp (Ferrari & Quaresima, 2012). In this study, the feasibility of using the Artinis Brite fNIRS system (Artinis, Medical Systems, The Netherlands) to simultaneously monitor

acute stress and brain activity is explored. This device takes measurements at high rates (up to 75/s) enabling the pulsatile changes in blood oxygenation to be gathered, which may be used to assess changes in the pulse amplitude, and thus SA, in the same manner as Udhayakumar et al. (2023).

To examine stress-induced sympathetic activation, two physiological and two cognitive stressors were selected: the cold pressor test (CPT), an isometric handgrip exercise, an unsolvable anagram task, and a color–shape interference task. The CPT is a well-established method used to induce SA and assess autonomic function by immersion of an extremity in cold water (Fanning et al., 2023). The resulting SA leads to an increased heart rate, arterial blood pressure and vascular resistance (Silverthorn & Michael, 2013). Isometric handgrip exercises also induce SA through both central and peripheral mechanisms, including cortical motor commands and the accumulation of metabolic byproducts. As a result, muscle sympathetic nerve activity (MSNA), vasoconstriction and arterial blood pressure increase (Costa & Biaggioni, 1994). An unsolvable anagram task was chosen because unsolvable problems give rise to a psychological feeling of uncontrollability. Demands that surpass an individual’s own perceived capabilities, which are unpredictable or uncontrollable, are able to induce a stress response (Starcke, Agorku, & Brand, 2017). The color-shape interference task, a variation of the classic Stroop task, tests the cognitive interference between naming one attribute of a stimulus (e.g. shape) with another attribute (e.g. color). Stroop tasks have shown to increase SA more effectively and consistently than other psychological stressors (Fechir et al., 2008).

In this study, we anticipate that all four stressor tasks will induce SA, which will be detectable in the hemodynamic signal captured by the fNIRS system. To assess this, we will analyze the AC component of the fNIRS signal using AvgSampEn and TotalSampEn, as

described by Udhayakumar et al. (2023). Given that SA is expected to reduce beat-to-beat variability in the signal, we hypothesize that the standard deviation of the signal will decrease during stress. Therefore, fewer tolerance thresholds (r-values) will fall within the entropy calculation range ( $0.1$  to  $0.25 \times \text{SD}$ , as outlined by Udhayakumar et al., 2017), leading to an increase in both AvgSampEn and TotalSampEn due to a greater proportion of signal irregularity being captured at these narrower tolerance thresholds.

## **Methods and Materials**

### **Participants**

A total of fifteen participants, both male and female, aged between 19 and 30, were recruited for this study. Participants were recruited through social media (e.g., instagram and facebook) and word of mouth. The inclusion criteria required participants to be between 18 - 39 years old, have normal or corrected-to-normal vision, and be fluent in English. The exclusion criteria included individuals who had a history of cardiovascular disease (e.g. previous heart attack, previous stroke, or were currently being treated for high blood pressure or high cholesterol), had been diagnosed as having type 1 or 2 diabetes or metabolic syndrome, had respiratory illnesses like chronic obstructive pulmonary disease, or had a cognitive disorder that may be related to vascular dysfunction (e.g. dementias). All participants gave informed consent prior to the commencement of any experimental procedures. Compensation for their participation was provided in the form of Tim Hortons or Starbucks gift cards valued at fifteen dollars.

### **Procedure**

Upon arrival at the lab, participants were assured of confidentiality (each was assigned a random number, with no identifying information recorded apart from the consent form). They were provided with a consent form outlining the study's purpose, procedures (including the estimated time commitment), potential risks and benefits, compensation, confidentiality assurances, the right to withdraw, and contact information. Participants who chose not to consent or later withdrew from the study were still compensated.

Participants were then instructed to perform three maximal hand grips using a hand grip force measurement device connected to an ADInstruments PowerLab 26T. The data was

recorded via LabChart software on a desktop computer. The first maximal hand grip was measured after 30 seconds, with the subsequent two grips separated by 30-second rest intervals. The maximal and minimal values (in mV) were then extracted from the data and used to set 100% and 0% force, respectively, for a later experiment.

#### ECG and ABP set-up

After completing the maximal hand grips, participants were equipped with devices to monitor both heart rate and blood pressure. Heart rate was measured using an electrocardiogram (ECG). Three electrodes were positioned on the participant: one just below the right clavicle, one below the left clavicle, and one just above the left hip, using 3M-2560 Red Dot Multi-Purpose Monitoring Electrodes (1000/cs). The positive lead was connected to the hip electrode, the ground to the left clavicle, and the negative lead to the right clavicle (as seen in figure one).

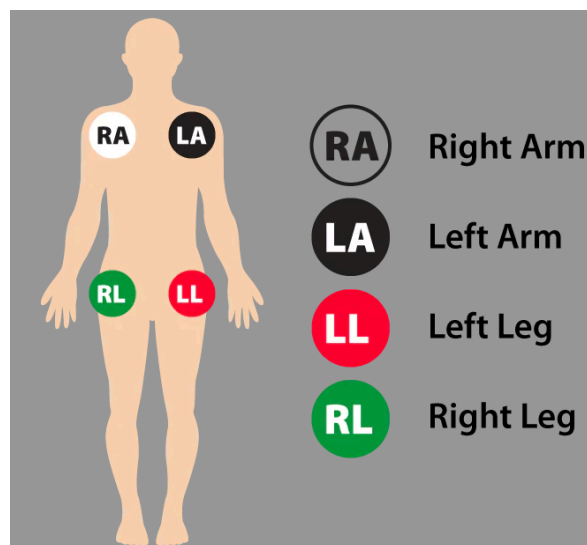


**Figure 1.** ECG set-up used (right leg excluded).

Arterial blood pressure (ABP) was measured using a CNAP monitor (CNSystems, Austria) that included an arm cuff and appropriately sized finger cuffs (small, medium, or large).



The arm cuff was applied first, followed by the finger cuffs, fitted according to the participant's finger size. Both blood pressure and heart rate data were recorded through Acqknowledge software on a laptop computer (Samsung series 7 Chronos) via the BIOPAC system.

### fNIRs set-up

After participants were equipped with blood pressure and heart rate monitors, they were then fitted with the Artinis Brite fNIRS head cap (Artinis, Medical Systems, The Netherlands). The neoprene cap was equipped with 10 light-emitting optodes, which transmitted near-infrared light in the 650-950 nm range, and 12 receivers that detected changes in light absorption, at a sampling rate of 75 Hz. The optodes were arranged in a 2 x 12 grid, spaced 3 cm apart, except for the short-separation channels, which were spaced 1.5 cm apart. This configuration created 24 recording channels which each continuously tracked fluctuations in the concentrations of oxygenated and deoxygenated hemoglobin. The fNIRS signal was recorded using OxySoft 4 software.

Once robust signals were ensured from the ECG, ABP, and fNIRS, participants completed two mental stress tasks and two physical stress tasks, with the order of tasks randomized for each participant. The randomization included both the sequence of the task categories—mental or physical—and the order of individual tasks within each category. Participants began in a seated position with their left hand, fitted with the ABP finger cuffs, resting on the arm of the chair, while their right hand remained free. They were asked to minimize movement and speech unless necessary to avoid disrupting any signals. A 10-minute rest period was conducted to establish baseline hemodynamic measurements, during which participants remained seated in the chair without engaging in any activity. After the 10-minute

rest period, participants undertook one of four tasks. Each cognitive stress task lasted five minutes, while the physical stress tasks were three minutes in duration. During the post-task period, participants were permitted to relax, while continuing to minimize movement and speech as much as possible. Following each task, a 10-minute rest period was mandated before the start of the subsequent task. Upon completing one category of tasks (either cognitive or physical), participants were provided with an opportunity to rest before proceeding to the next category.

### Mental Stress Tasks

The two cognitive stress tasks included an unsolvable anagram and a color–shape interference task, both derived from the millisecond test library within the Inquisit 5 software. Each task was presented to participants on a laptop (MacBook Air 2020, 13”, 2560 x 1600 resolution), and they were instructed to only use their free hand. Both tasks were limited to a duration of five minutes, regardless of the participants progress, and including the practice trial.

The unsolvable anagrams task involved presenting participants with a series of scrambled letters (see figure two) that could and could not be arranged into meaningful words, at random intervals, within a thirty second time limit. The practice trial consisted of five solvable anagrams. Following the practice trial, participants were prompted with a message informing them they had to unscramble twenty-five letter sets into meaningful words and that they would pass if they solved at least eight of the twenty-five words or fail if they solved seven or fewer. Unbeknownst to the participants, not all the scrambled letter combinations could form meaningful words. During the debriefing session following the experiment, participants were informed of this.

# COELPU

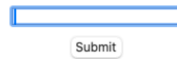


**Figure 2.** An example of a scrambled letter combination presented to participants, who had thirty seconds to solve it before the screen switched to the next anagram.

The color–shape interference task involved presenting participants with shapes that varied in color and form (figure three). Each shape and color was associated with a specific key on the laptop: the key 'A' corresponded to a circle and the color red, while 'L' corresponded to a triangle and the color green. Participants were required to press the designated key based on specific rules that varied throughout the task.

During the initial practice block, participants were shown shapes without color and instructed to identify the shape. In the subsequent practice block, they were presented with colored squares and asked to identify the color. In the post-practice block one, participants were shown shapes (circle or triangle) or colored squares and were instructed to identify either the shape when no color was present, or the color when it was present. In post-practice block two, participants were shown shapes superimposed on coloured squares and asked to identify the color when it was red or the shape if it was green. The blocks became increasingly difficult as they progressed however, most participants only made it to post-practice block two with the five-minute time limit. Consistent with the unsolvable anagrams task, participants were permitted to use only their free hand.

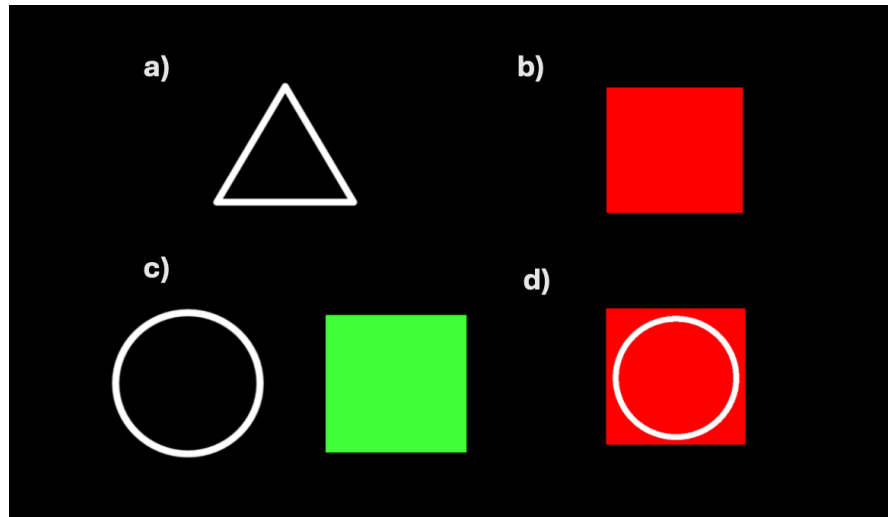


**Figure 3. Examples of images presented in the color–shape interference task.** In the upper left (a), one of the two shapes from practice block one is depicted. The upper right (b) illustrates one of the two colors featured in practice block two. The lower left (c) presents two instances requiring participants to choose between shape or color in post-practice block one. Finally, the lower right (d) displays an example of a superimposed image from post-practice block two, where the correct answer is red.

### Physical Stress Tasks

The physical stress tasks consisted of a isometric handgrip task and a CPT, each lasting three minutes. For the isometric handgrip task, an MLT004/ST Grip Force Transducer connected to a PowerLab system (ADInstruments, New Zealand) was utilized. Participants were seated with the transducer in their dominant hand, facing a desktop computer displaying the lab chart output. They were instructed to maintain a grip force at 20% of their maximal handgrip strength, which was determined at the start of the experiment, for the duration of three minutes. The exerted percentage and a three-minute timer were visible on the computer screen. Upon

completion, participants were asked to release the transducer and remain as still as possible while the researcher removed the device from their hand.

The CPT involved the participant submerging their hand in water maintained at a temperature of 3-5°C for three minutes (Silverthorn & Michael, 2013). A four-quart stainless steel mixing bowl was filled to approximately three-quarters capacity with room-temperature water, and ice was added until the water temperature reached the desired range, as measured with a digital thermometer. The participant remained seated and placed their free hand into the bowl positioned beside them. To prevent the formation of a thermal layer, the researcher continuously stirred the water. At the end of the three-minute period, the researcher removed the participant's hand and gently dried it with a paper towel to minimize participant movement.

### **Statistical Analysis**

All data were analyzed across the same two time periods for each of the four tasks for every participant. These included a three-minute pre-task rest period that began four minutes before task onset, and the first three minutes of the task itself, labeled as the 'pre' and 'during' periods, respectively. A linear mixed model was used to analyze all data due to its flexibility in accounting for both fixed and random effects. This method was suitable given that not all participants completed every task, as it can handle missing data without listwise deletion. Jeffrey's Amazing Statistics Program (JASP) was used to perform all linear mixed model analyses and flexplots.

### **ABP Data**

Arterial blood pressure data for each participant was analyzed using AcqKnowledge software. For instances where the 'pre' period of the ABP signal was disrupted (e.g. excessive

artifacts or during recalibration periods), the analyzed 'pre' segment was adjusted to include the three minutes immediately prior to the disruption.

AvgSampEn and TotalSampEn values were analyzed from the ABP data using AcqKnowledge and MATLAB software. Within AcqKnowledge, a low-pass filter was applied to reduce artifacts and preserve physiological waveform features. The 'Hemodynamics— Arterial Blood Pressure' analysis module was used to extract physiological metrics from the BP waveform, which detects individual cardiac cycles based on systolic and diastolic markers in the waveform. These metrics, including pulse height and heart rate, were exported to Excel for further analysis. To ensure data quality, pulse height values were cross-referenced with the heart rate values, and any data points associated with implausibly high heart rate readings (due to signal artifacts) were excluded. Corresponding pulse height values were removed to eliminate artifact-related distortions from the analysis. Pulse height data were exported as a text file and imported into MATLAB, where AvgSampEn and TotalSampEn values were computed and recorded in an Excel spreadsheet (see appendix A for MATLAB code). This data were then exported from Excel as a text file and imported into JASP for statistical analysis.

Mean arterial pressure (MAP) values were extracted from the 'pre' and 'during' time periods for each task for every participant. These values were obtained from the blood pressure metrics Excel sheet, generated using the 'Hemodynamics – Arterial Blood Pressure' module in AcqKnowledge. The MAP values were recorded into a separate Excel file, exported as a text file, and subsequently imported into JASP for statistical analysis.

### fNIRS Data

The fNIRS signal was recorded using OxySoft 4 software and exported into a SNIRF file, then imported into MATLAB using the Brain AnalyzIR Toolbox. Preprocessing began by scaling the optode coordinate system and relabeling sources and detectors for clarity. The data were then converted to optical density and further transformed into concentrations of oxyhemoglobin and deoxyhemoglobin using the modified Beer-Lambert law (see appendix B for MATLAB code). A subset of six fNIRS channels were selected for evaluation (channels 15, 17, 23, 39, 43, and 45). A custom MATLAB script performed spectral analysis and signal filtering to isolate pulse waveforms from each selected channel during the previously determined time periods (pre and during tasks). Peaks were identified and their prominence values were extracted over time, and used to compute AvgSampEn and TotalSampEn values (see appendix C for MATLAB code). AvgSampEn and TotalSampEn were recorded for each channel, during each time period, across all four tasks, for every participant in an excel spreadsheet. This data were then exported from Excel as a text file and imported into JASP for statistical analysis.

## Results

### fNIRS

fNIRS TotalSampEn significantly increased from Pre to During task ( $p = 0.036$ ) and similarly for AvgSampEn ( $p = 0.023$ , as seen in figures 4 and 5, respectively). There were no significant differences among tasks and no significant task  $\times$  time interaction observed ( $p > 0.05$ ).

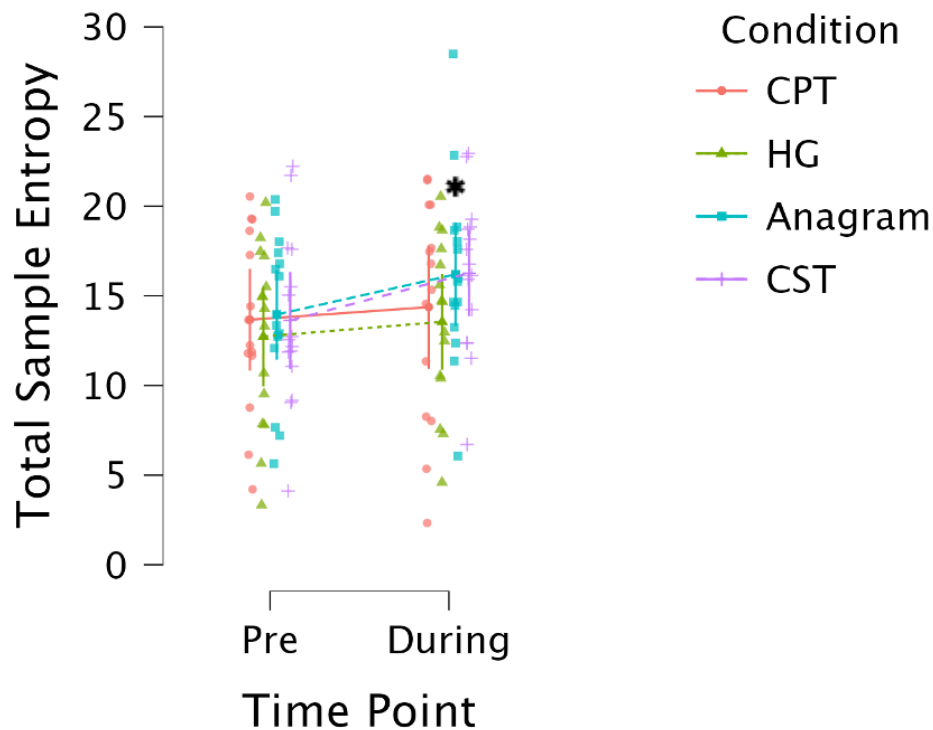


**Figure 4.** Comparison of fNIRS TotalSampEn pre- and during-task engagement across all four tasks (Anagram, CST, HG, CPT). The \* indicates a significant ( $p = 0.036$ ) increase in TotalSampEn from pre- to during- task, with no significant difference among task types ( $p > 0.05$ ). ( $n = 15$ )



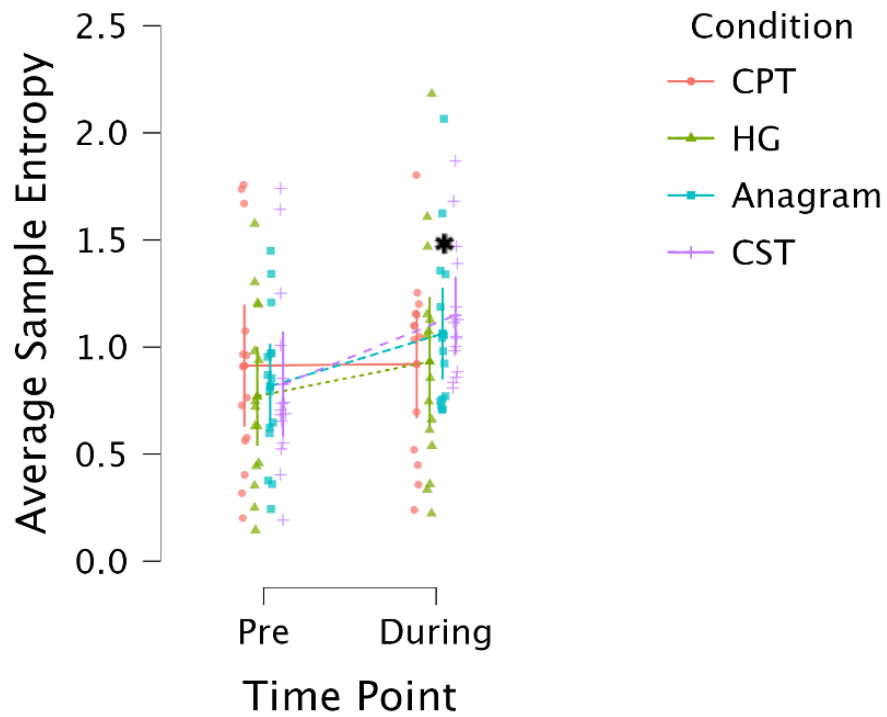


**Figure 5.** Comparison of fNIRS AvgSampEn pre- and during-task engagement across all four tasks (Anagram, CST, HG, CPT). The \* indicates a significant ( $p = 0.023$ ) overall increase in AvgSampEn from pre- to during- task, with no significant difference among task types ( $p > 0.05$ ). ( $n = 15$ )

## Blood Pressure

Mean arterial pressure (MAP) significantly increased from pre- to during-task engagement across all four tasks as seen in figure 6 ( $p = 0.005$ ). There were no significant differences among tasks and no significant task  $\times$  time interaction, indicating a uniform increase in MAP across all conditions ( $p > 0.05$ ).

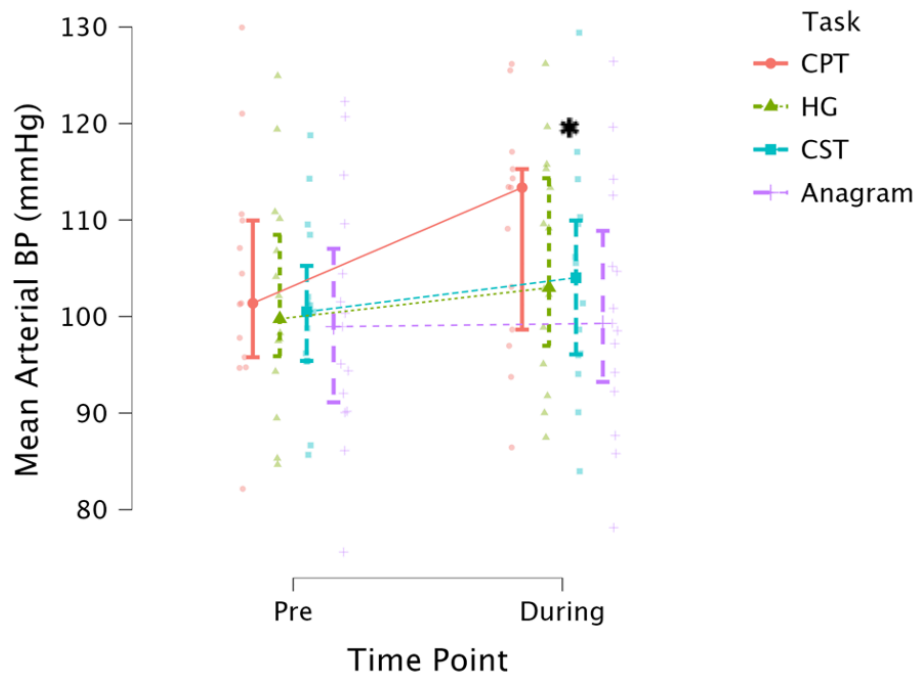


**Figure 6.** Comparison of mean arterial pressure (MAP) pre- and during-task engagement across all four tasks (Anagram, CST, HG, CPT). The \* indicates a significant ( $p = 0.005$ ) increase in MAP from pre- to during-task with no significant difference among task types ( $p > 0.05$ ). (n = 15)

As shown in figure 7, blood pressure AvgSampEn showed a significant main effect of task ( $p = 0.014$ ) and time ( $p = 0.009$ ), as well as a significant task  $\times$  time interaction ( $p = 0.002$ ). The largest increase occurred during the Anagram task (Pre: 0.507  $\rightarrow$  During:

0.89,  $p < 0.001$ ), followed by HG ( $p = 0.013$ ), and CST ( $p = 0.049$ ). CPT showed a non-significant decrease ( $p > 0.05$ ).

Blood pressure TotalSampEn trended towards significance for the main effects of Task ( $p = 0.056$ ) and Time ( $p = 0.052$ ) although these effects did not meet conventional thresholds for statistical significance ( $p < 0.05$ ). However, TotalSampEn showed a significant task  $\times$  time interaction ( $p = 0.0014$ ), with only the Anagram showing a significant increase from Pre to During, as seen in figure 8 ( $p = 0.029$ ). Other tasks showed non-significant trends ( $p > 0.05$ ).

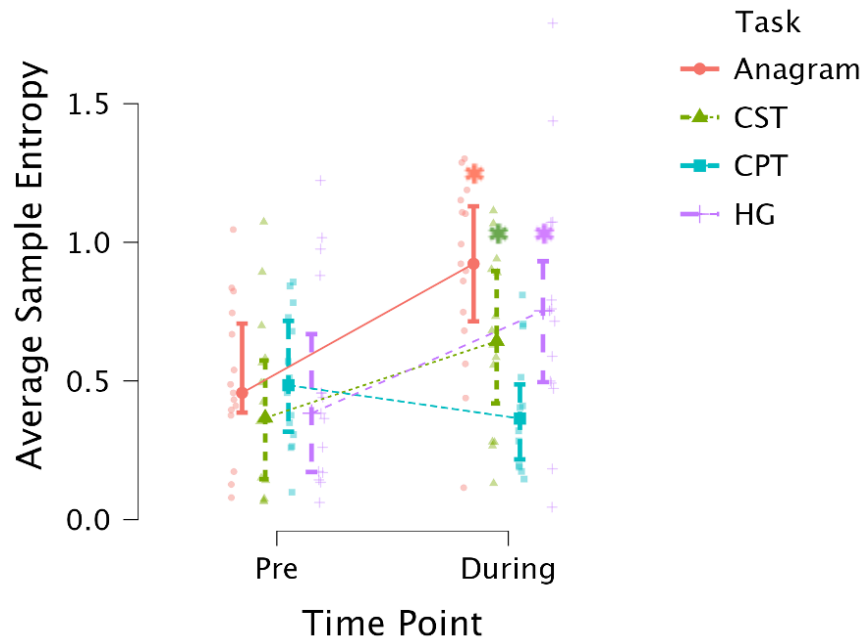


**Figure 7.** Comparison of blood pressure AvgSampEn pre- and during-task engagement across all four tasks (Anagram, CST, HG, CPT). The \* indicates the significant main effects of task  $\times$  time interactions ( $p = 0.002$ ). The largest increase was observed during the Anagram task (Pre: 0.507  $\rightarrow$  During: 0.891,  $p < 0.001$ ), followed by HG ( $p = 0.013$ ) and CST ( $p = 0.049$ ). CPT showed a non-significant decrease ( $p = 0.277$ ). ( $n = 15$ )

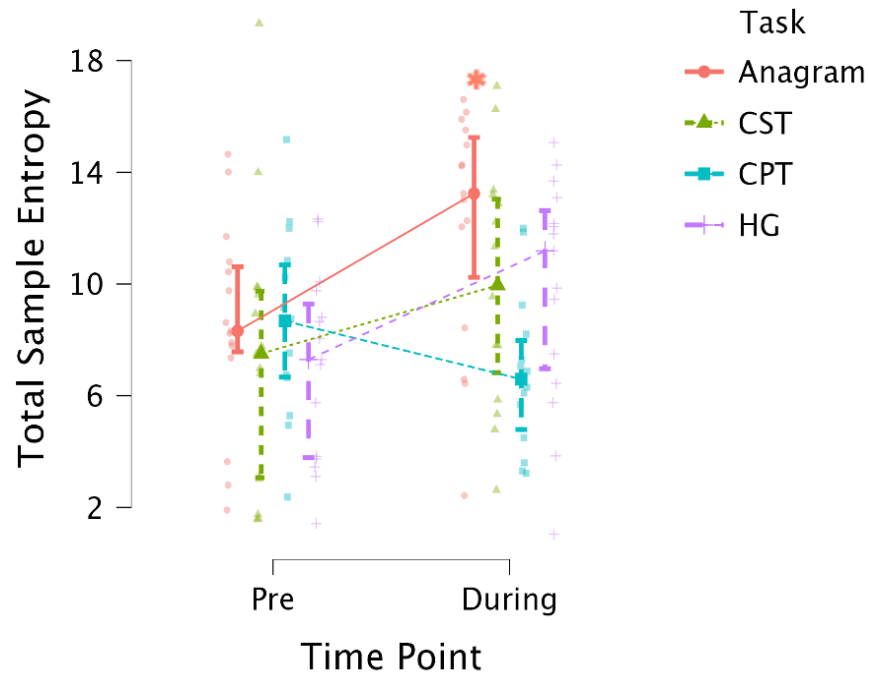


**Figure 8.** Comparison of blood pressure TotalSampEn pre- and during-task engagement across all four tasks (Anagram, CST, HG, CPT). The \* indicates a significant task  $\times$  time interaction ( $p = 0.014$ ), with only the Anagram task showing a statistically significant increase in entropy from pre- to during-task engagement ( $p = 0.029$ ). Other tasks exhibited non-significant trends ( $p > 0.05$ ). ( $n = 15$ )

## Discussion

### Main Findings

This study investigated whether physiological and cognitive stressor induced SA could be captured through entropy-based pulsatile changes in fNIRS signals while simultaneously monitoring brain activity. SA was seen by a significant increase in mean arterial pressure (MAP) across all tasks ( $p = 0.0005$ ) from pre- to during-task engagement. Given that MAP increases with activation of the sympathetic nervous system, due to vasoconstriction and increased cardiac output, implies the stressor tasks were successful in inducing SA (Silverthorn & Michael, 2013). However, the blood pressure entropy data showed more nuanced results. The change in AvgSampEn entropy over time depended on which task the individual was doing. Overall AvgSampEn increased significantly pre- to during-task engagement across most tasks, particularly Anagram, Handgrip, and Color-Shape Interference tasks from most to least ( $p < 0.001$ ,  $p = 0.013$ ,  $p = 0.049$ , respectively). However, the CPT AvgSampEn did not change significantly from pre- to during-task engagement. It is possible that the CPT induced a large sympathetic response initially, which increased muscle sympathetic nerve activity (MSNA), increasing MAP and inducing an arterial baroreflex response to counteract the rise in pressure (Cui et al., 2001). Since AvgSampEn was taken over the entire three minutes of the CPT that could have allowed the body time to adjust, increasing variability of the AC component over time and reducing AvgSampEn changes. Minute-by-minute entropy analysis may provide more precise insights into how SA evolves during prolonged stress exposure.

In contrast to AvgSampEn, blood pressure TotalSampEn showed a less consistent pattern across tasks. There was a significant task by time interaction observed ( $p = 0.0014$ ) with the Anagram task being the only task to show significance: an increase in TotalSampEn from pre- to during-task engagement ( $p = 0.029$ ). However, when comparing results of TotalSampEn to

Udhayakumar et al. 2013, notable differences emerge, particularly in how TotalSampEn fluctuated on a minute-by-minute basis. In their study, entropy decreased during the first minute of stress exposure, followed by a progressive increase in the second minute and recovery. This finding highlights how averaging entropy across the entire stress period may hide temporal shifts in SA, which could help lead to more conclusive results.

In agreement with our hypothesis, both AvgSampEn and TotalSampEn derived from the fNIRS signal increased significantly from pre- to during-task engagement ( $p = 0.023$ ,  $p = 0.036$ ) across all four tasks. However, there was no significant task by time interaction observed in the fNIRS data, suggesting that the increase in entropy was uniform regardless of the stressor. This uniform increase could be because SA produces a generalized effect on cerebral blood flow, leading to uniform increases in entropy, in contrast to more variable entropy patterns observed in peripheral blood flow. Despite sympathetic innervation, the SNS does not contribute largely to cerebral blood flow dynamics unlike chemical and metabolic controls (ter Laan et al., 2013). When it does, it tends to limit blood flow similarly in response to any stressors, which could indicate the response may not vary much between stressors. These findings support the feasibility of using fNIRS to assess SA by measuring AvgSampEn through the AC component of the hemodynamic signal, offering a non-invasive and objective approach to monitoring psychological stress.

### **Sources of Error and Limitations**

There are several limitations to consider when interpreting the findings of this research. First, the study was conducted in a laboratory setting, utilizing physiological and cognitive stressors that are known to reliably induce SA. However, real-life stressors or anxiety may

produce more subtle sympathetic activity which may not be detectable via pulsatile changes in the signal. The generalizability of these findings to other settings remains uncertain. Second, the sample population consisted entirely of healthy young adults, limiting the applicability of the findings to more diverse populations. Physiological responses to stress may change with age as older adults experience vascular stiffening, hypertension, and/or autonomic dysfunction (Zieman et al., 2015; Parashar et al., 2016). Additional research would be needed to assess if this assessment of SA is viable in older populations. Third, SA was determined indirectly through only one physiological response (increased MAP). While this response may be supported by the literature, it is only one measure, and it is not a direct measurement of sympathetic nervous system activity. The absence of direct measurements limits the ability to attribute the observed entropy changes to SA alone.

### **Future Research**

Several directions for future research are recommended to build on the current findings. As mentioned previously, future studies should assess minute-by-minute analyses of AvgSampEn and TotalSampEn throughout the pre-task, task, and recovery periods. Previous research has shown that entropy values may fluctuate within short time windows after stress onset (Udhayakumar, 2023). Averaging entropy over longer segments may obscure important phase-specific changes in SA, which can be time-sensitive. Future studies should also include additional physiological measurements to validate SA, in addition to MAP. These may include pulse transmit time (PTT) and heart rate (HR). PTT serves as an indicator of arterial stiffness which increases during vasoconstriction under sympathetic influence, thus decreasing PTT (Weiss et al., 1980; Zhang et al., 2011). HR can be used as a covariate, as higher HR reduces

ventricular filling time during diastole, limiting the stroke volume fluctuations respiratory sinus arrhythmia (RSA) would normally induce (Kerr et al., 1998). Including these variables could allow for correlational analyses between entropy and sympathetic activity. Additionally, future work should aim to include direct measurements of sympathetic nervous system activity. Direct measurements can be monitored through sympathetic microneurography, which involves placing a needle in the efferent axon of a sympathetic nerve (White et al., 2015). This measurement would make it possible to conclude sympathetic outflow was achieved. SA could also be assessed via biochemical assays to measure circulating catecholamines such as epinephrine and norepinephrine (Christensen, 1990).

Finally, future research could incorporate pharmacological antagonists to better understand how changes in entropy are modulated by sympathetic versus parasympathetic branches of the ANS (thus mimicking stress versus relaxed environments). Using antagonists such as beta-adrenergic blockers, which prevent norepinephrine from binding to  $\beta$ -receptors (therefore blocking SA), allows researchers to observe parasympathetic activity in isolation (Aronson and Burger, 2001). This would help clarify whether observed entropy changes are primarily driven by stress-induced sympathetic activation.



### Literature Cited

- Aronson, D., & Burger, A. J. (2001). Effect of beta-blockade on autonomic modulation of heart rate and neurohormonal profile in decompensated heart failure. *Annals of Noninvasive Electrocardiology*, 6(2), 98–106. <https://doi.org/10.1111/j.1542-474X.2001.tb00093.x>
- Bigalke, J. A., Durocher, J. J., Greenlund, I. M., Keller-Ross, M., & Carter, J. R. (2023). Blood pressure and muscle sympathetic nerve activity are associated with trait anxiety in humans. *American Journal of Physiology-Heart and Circulatory Physiology*, 324(5), H494–H503. <https://doi.org/10.1152/ajpheart.00026.2023>
- Cables and Sensors. (n.d.-a). 12-lead ECG placement: The ultimate guide. Cables and Sensors. <https://www.cablesandsensors.com/pages/12-lead-ecg-placement-guide-with-illustrations>
- Cui, J., Wilson, T. E., Shibasaki, M., Hodges, N. A., & Crandall, C. G. (2001). Baroreflex modulation of muscle sympathetic nerve activity during posthandgrip muscle ischemia in humans. *Journal of Applied Physiology*, 91(4), 1679–1686. <https://doi.org/10.1152/jappl.2001.91.4.1679>
- Costa, F., & Biaggioni, I. (1994). Role of adenosine in the sympathetic activation produced by isometric exercise in humans. *Journal of Clinical Investigation*, 93(4), 1654–1660. <https://doi.org/10.1172/JCI117147>
- Eysenck, M. W., Derakshan, N., Santos, R., & Calvo, M. G. (2007). Anxiety and cognitive performance: Attentional control theory. *Emotion*, 7(2), 336–353. <https://doi.org/10.1037/1528-3542.7.2.336>

Christensen, N.J. (1990). The biochemical assessment of sympathoadrenal activity in man.

*Baillière's Clinical Endocrinology and Metabolism*, 4(3), 403–424.

<https://doi.org/10.1007/BF01826215>

Fanning, S., Plener, P. L., Fischer, M. J. M., Kothgassner, O. D., & Goreis, A. (2023). Water temperature during the cold pressor test: A scoping review. *Physiology & Behavior*, 271, 114354. <https://doi.org/10.1016/j.physbeh.2023.114354>

Fechir, M., Schlereth, T., Purat, T., Kritzmman, S., Geber, C., Eberle, T., Gamer, M., & Birklein, F. (2008). Patterns of sympathetic responses induced by different stress tasks. *The Open Neurology Journal*, 2, 25–31. <https://doi.org/10.2174/1874205X00802010025>

Ferrari, M., & Quaresima, V. (2012). A brief review on the history of human functional near-infrared spectroscopy (fNIRS) development and fields of application. *NeuroImage*, 63(2), 921–935. <https://doi.org/10.1016/j.neuroimage.2012.03.049>

Kerr, A. J., Simmonds, M. B., & Stewart, R. A. (1998). Influence of heart rate on stroke volume variability in atrial fibrillation in patients with normal and impaired left ventricular function. *American Journal of Cardiology*, 82(12), 1496–1500. [https://doi.org/10.1016/s0002-9149\(98\)00693-6](https://doi.org/10.1016/s0002-9149(98)00693-6)

Kim, S. W., Lee, D., Kim, J. H., Lee, J., Kang, D. H., Kim, S.-Y., & Choi, S.-H. (2025). Autonomic readiness for social threats in patients with social anxiety disorder. *Clinical Psychopharmacology and Neuroscience*, 23(2), 202–211. <https://doi.org/10.9758/cpn.24.1228>

- Macefield, V. G. (2021). Recording and quantifying sympathetic outflow to muscle and skin in humans: Methods, caveats and challenges. *Clinical Autonomic Research*, 31(1), 59–75. <https://doi.org/10.1007/s10286-020-00700-6>
- Meissel, K., & Salthouse, T. A. (2016). Relations of naturally occurring variations in state anxiety and cognitive functioning. *Personality and Individual Differences*, 98, 85–90. <https://doi.org/10.1016/j.paid.2016.04.018>
- Moran, T. P. (2016). Anxiety and working memory capacity: A meta-analysis and narrative review. *Psychological Bulletin*, 142(8), 831–864. <https://doi.org/10.1037/bul0000051>
- Naveh-Benjamin, M., McKeachie, W. J., Lin, Y.-g., & Holinger, D. P. (1981). Test anxiety: Deficits in information processing. *Journal of Educational Psychology*, 73(6), 816–824. <https://doi.org/10.1037/0022-0663.73.6.816>
- Parashar, R., Amir, M., Pakhare, A., Rathi, P., & Chaudhary, L. (2016). Age related changes in autonomic functions. *Journal of Clinical Gerontology and Geriatrics*, 7(2), 65–69. <https://doi.org/10.1016/j.jcgg.2016.01.003>
- Richards, J. C., & Bertram, S. (2000). Anxiety sensitivity, state and trait anxiety, and perception of change in sympathetic nervous system arousal. *Journal of Anxiety Disorders*, 14(4), 413–427. [https://doi.org/10.1016/S0887-6185\(00\)00031-1](https://doi.org/10.1016/S0887-6185(00)00031-1)
- Salthouse, T. A. (2012). Consequences of age-related cognitive declines. *Annual Review of Psychology*, 63, 201–226. <https://doi.org/10.1146/annurev-psych-120710-100328>

- Silverthorn, D. U., & Michael, J. (2013). Cold stress and the cold pressor test. *Advances in Physiology Education*, 37(1), 93–96. <https://doi.org/10.1152/advan.00104.2012>
- Starcke, K., Agorku, J. D., & Brand, M. (2017). Exposure to unsolvable anagrams impairs performance on the Iowa Gambling Task. *Frontiers in Behavioral Neuroscience*, 11, 114. <https://doi.org/10.3389/fnbeh.2017.00114>
- ter Laan, M., van Dijk, J. M. C., Elting, J. W. J., Staal, M. J., & Absalom, A. R. (2013). Sympathetic regulation of cerebral blood flow in humans: A review. *British Journal of Anaesthesia*, 111(3), 361–367. <https://doi.org/10.1093/bja/aet122>
- Udhayakumar, R. K., Karmakar, C., & Palaniswami, M. (2017). Approximate entropy profile: A novel approach to comprehend irregularity of short-term HRV signal. *Nonlinear Dynamics*, 88(2), 823–837. <https://doi.org/10.1007/s11071-016-3278-z>
- Udhayakumar, R., Rahman, S., Buxi, D., Macefield, V. G., Dawood, T., Mellor, N., & Karmakar, C. (2023). Measurement of stress-induced sympathetic nervous activity using multi-wavelength PPG. *Royal Society Open Science*, 10, 221382. <https://doi.org/10.1098/rsos.221382>
- Udina, C., Avtzi, S., Durduran, T., Holtzer, R., Rosso, A. L., Castellano-Tejedor, C., Perez, L.-M., Soto-Bagaria, L., & Inzitari, M. (2019). Functional near-infrared spectroscopy to study cerebral hemodynamics in older adults during cognitive and motor tasks: A review. *Frontiers in Aging Neuroscience*, 11, 367. <https://doi.org/10.3389/fnagi.2019.00367>

- White, D. W., Shoemaker, J. K., & Raven, P. B. (2015). Methods and considerations for the analysis and standardization of assessing muscle sympathetic nerve activity in humans. *Autonomic Neuroscience*, 193, 12–21. <https://doi.org/10.1016/j.autneu.2015.08.004>
- Weiss, T., Del Bo, A., Reichek, N., & Engelman, K. (1980). Pulse transit time in the analysis of autonomic nervous system effects on the cardiovascular system. *Psychophysiology*, 17(2), 202–207. <https://doi.org/10.1111/j.1469-8986.1980.tb00136.x>
- Zhang, Y.-L., Zheng, Y.-Y., Ma, Z.-C., & Sun, Y.-N. (2011). Radial pulse transit time is an index of arterial stiffness. *Hypertension Research*, 34, 884–887. <https://doi.org/10.1038/hr.2011.74>
- Zieman, S. J., Melenovsky, V., & Kass, D. A. (2015). Age-related vascular stiffening: Causes and consequences. *Frontiers in Genetics*, 6, 112. <https://doi.org/10.3389/fgene.2015.00112>

## Appendix A

### MATLAB Code for Blood Pressure ASE & SE

```
peak_prominence = Data;  
%Extract pulse related data (height, slope, from each Stim (25 beats prior to  
40 beats  
%afterwards)  
r_values = (0.35:0.01*std(peak_prominence):0.25*std(peak_prominence)); %to  
obtain a range of relevant r's to use in the sample entropy  
%Calculate SampEn of the segment with a r= 0.15 *sd and a tolerance of m=2  
saen2 = total_sample_entropy(peak_prominence,2,r_values);  
avgsampentropy = saen2/(length(r_values));
```

## Appendix B

### MATLAB Code for fNIRS Preprocessing

```
%Load the snirf files
raw = nirs.io.loadSNIRF('modified snirf file');
%modify the formatting of the loaded Raw file for subsequent steps
chan=24*2;%input the number of channels - multiplied by two for oxy and deoxy
temp = zeros(chan,1);
idx = [6 21 30 45]; %change these depending on which are your short channels
(must know in advance which source and detector but also which rows in the
probe.linkObj file (or you can find it using script)
for i = 1:4
temp(idx,1) = 1; %loops and adds the value "1" at the correct rows of the temp
variable to be inserted as the shortchannel information
end
for i = 1:(length(raw))
raw(i, 1).probe.optodes_registered.Y = raw(i,1).probe.optodes_registered.Y *
10;
raw(i, 1).probe.optodes_registered.X = raw(i,1).probe.optodes_registered.X *
10;
raw(i, 1).probe.optodes.Y = raw(i, 1).probe.optodes.Y * 10;
raw(i, 1).probe.optodes.X = raw(i, 1).probe.optodes.X * 10;
raw(i, 1).probe.optodes.Name{1} = 'Source-01';
raw(i, 1).probe.optodes.Name{2} = 'Source-02';
raw(i, 1).probe.optodes.Name{3} = 'Source-03';
raw(i, 1).probe.optodes.Name{4} = 'Source-04';
raw(i, 1).probe.optodes.Name{5} = 'Source-05';
raw(i, 1).probe.optodes.Name{6} = 'Source-06';
raw(i, 1).probe.optodes.Name{7} = 'Source-07';
raw(i, 1).probe.optodes.Name{8} = 'Source-08';
raw(i, 1).probe.optodes.Name{9} = 'Source-09';
raw(i, 1).probe.optodes.Name{10} = 'Source-10';
raw(i, 1).probe.optodes.Name{11} = 'Detector-01';
raw(i, 1).probe.optodes.Name{12} = 'Detector-02';
raw(i, 1).probe.optodes.Name{13} = 'Detector-03';
raw(i, 1).probe.optodes.Name{14} = 'Detector-04';
raw(i, 1).probe.optodes.Name{15} = 'Detector-05';
raw(i, 1).probe.optodes.Name{16} = 'Detector-06';
raw(i, 1).probe.optodes.Name{17} = 'Detector-07';
raw(i, 1).probe.optodes.Name{18} = 'Detector-08';
raw(i, 1).probe.optodes_registered.Name{1} = 'Source-01';
raw(i, 1).probe.optodes_registered.Name{2} = 'Source-02';
raw(i, 1).probe.optodes_registered.Name{3} = 'Source-03';
raw(i, 1).probe.optodes_registered.Name{4} = 'Source-04';
raw(i, 1).probe.optodes_registered.Name{5} = 'Source-05';
raw(i, 1).probe.optodes_registered.Name{6} = 'Source-06';
raw(i, 1).probe.optodes_registered.Name{7} = 'Source-07';
```

```

raw(i, 1).probe.optodes_registered.Name{8} = 'Source-08';
raw(i, 1).probe.optodes_registered.Name{9} = 'Source-09';
raw(i, 1).probe.optodes_registered.Name{10} = 'Source-10';
raw(i, 1).probe.optodes_registered.Name{11} = 'Detector-01';
raw(i, 1).probe.optodes_registered.Name{12} = 'Detector-02';
raw(i, 1).probe.optodes_registered.Name{13} = 'Detector-03';
raw(i, 1).probe.optodes_registered.Name{14} = 'Detector-04';
raw(i, 1).probe.optodes_registered.Name{15} = 'Detector-05';
raw(i, 1).probe.optodes_registered.Name{16} = 'Detector-06';
raw(i, 1).probe.optodes_registered.Name{17} = 'Detector-07';
raw(i, 1).probe.optodes_registered.Name{18} = 'Detector-08';
raw(i, 1).probe.link.ShortSeperation = temp;
end
clear temp;
%convert to hb from raw
jobs=nirs.modules.OpticalDensity(); %converts raw data to optical density
jobs=nirs.modules.BeerLambertLaw(jobs); %applies Beer-Lambert to get Hb
hb=jobs.run(raw);

```



## Appendix C

### MATLAB Code for fNIRS SE & ASE

```

%% Analyzing the pulse of fNIRS datasets while under stress
% Cleaning of fNIRS data to extract peaks and troughs
% Calculating the Pulse amplitudes over time
% Incorporation of SampEn to assess changes in entropy over time
% Identifying rapid changes in SampEn to indicate changes in SNS activation
% Steps in code development
% 1. Import the dataset using the Brain AnalyzIR toolkit from snirfs
% 2. Convert to Hb and trim data set
% 3. Possibly use the SNI to identify useful channels with structured noise
% which would be worth assessing
% 4. Pre-processing steps will involve:
% a. calculating the power spectrum of
% the signal,
% b. then identifying the maximal power within the spectrum of
% 0.6-3Hz, which would ID HRs of between 36-180bpm
% c. Apply a centre median and centre moving average filter to the
% data with a window size of 0.2*Peak-to-peak duration
% Load the .mat file
%Ignore data = load('nirs_example.mat');
hb_data = hb.data;
stimtime = 1023; % edit to the stimulus you are interested in
fs = 50;%specify the sampling frequency that the hb data is in
column_range = [15, 17, 23, 39, 43, 45]; % all the columns you want to run
entropy upon
stim_start_range = stimtime * fs; %enter the stimulus time you want to extract
from the HB data for this measure of entropy
hb_entropy_data =
hb_data(stim_start_range:(stim_start_range+(180*50)),column_range); % this is
the data before the stimulus
% Initialize structures to store results
peak_amplitudes = struct;
%relative_peak_amplitudes = struct;
peak_locations = struct;
peak_prominence = struct;
%baselines_all = struct;
% Process each column in hb_data
for col = 1:size(hb_entropy_data, 2)
% Extract the current column data
data_col = hb_entropy_data(:, col);
% Step 1: Calculate the power spectrum
n = length(data_col);
f = (0:n-1)*(fs/n); % Frequency vector
fft_col = fft(data_col);
power_spectrum = abs(fft_col).^2 / n;

```

```

% Step 2: Identify the maximal power within the spectrum of 0.5-3Hz
freq_range = find(f >= 0.5 & f <= 3);
[max_power, max_index] = max(power_spectrum(freq_range));
max_freq = f(freq_range(max_index));
% Calculate the peak-to-peak duration based on the identified HR frequency
peak_to_peak_duration = 1/max_freq;
% Step 3: Apply a central median and central moving average filter
window_size = round(0.2 * peak_to_peak_duration * fs);
filtered_median = medfilt1(data_col, window_size);
filtered_cma = movmean(filtered_median, window_size);
filtered_cma_invert = -1*filtered_cma;
% Step 4: Apply a 3rd order low pass Butterworth filter to create a
% % baseline signal to use to calculate relative peak heights
% [b, a] = butter(3, 0.5 * peak_to_peak_duration / (fs/2), 'low');
% baseline_filtered = filtfilt(b, a, filtered_cma);
% Detect peaks and troughs in the filtered data
[peaks, locs, w, p] = findpeaks(filtered_cma, 'Annotate', 'extents',
'MinPeakDistance', round(0.5 * fs)); %adjust the 0.5 (120bpm) to ensure all
peaks are identified
%[troughs, locst] = findpeaks(filtered_cma_invert, 'MinPeakDistance', round(0.5
*fs));
% Calculate relative peak heights from the peak and trough data
% relative_peaks = zeros(size(peaks));
% for i = 1:length(locs) % Find difference between the peak and trough of the
local peak
% relative_peaks(i) = peaks(i) - troughs(i);
% end
% Store results in structures
peak_amplitudes.(['col' num2str(col)]) = peaks;
%trough_amplitudes.(['col' num2str(col)]) = troughs;
% relative_peak_amplitudes.(['col' num2str(col)]) = relative_peaks;
peak_locations.(['col' num2str(col)]) = locs;
peak_prominence.(['col' num2str(col)]) = p;
% trough_locations.(['col' num2str(col)]) = locst;
% filtered_baseline(:,col) = baseline_filtered;
cma_filtered(:,col) = filtered_cma;
%cma_filtered_invert(:,col) = filtered_cma_invert;
% baselines_all.(['col' num2str(col)]) = relative_baseline;
end
%Determine the peak amplitudes by taking the peak locations and comparing
%them to the trough locations and if they are troughs are within 5 points
%before the peak, then a peak amplitude is calculated and placed in a
% %struct
% i=1
% for fieldNumber = 1:42
% fieldName = sprintf('col%d', fieldNumber); % Generate the field name
dynamically
% fieldValue = myStruct.(fieldName); % Access the field value
% % Do something with fieldValue

```

```

% disp(['Value of ', fieldName, ': ', num2str(fieldValue)]);
% end
% % Display the relative peak amplitudes for the first column as an example
% fprintf('Relative Peak Amplitudes for Column 1:\n');
% disp(relative_peak_amplitudes.col1);
% Uncomment the following section to plot specific column peaks
% time = (0:length(data_col)-1) / fs;
% col_to_plot = 1; % Change this to plot a different column
% findpeaks(cma_filtered(:,col_to_plot),'Annotate', 'extents',
'MinPeakDistance', round(0.5 * fs),'MaxPeakWidth',(2 * fs));
% figure;
% plot(time, cma_filtered(:, col_to_plot));
% hold on;
% plot(peak_locations.(['col' num2str(col_to_plot)]) / fs,
peak_amplitudes.(['col' num2str(col_to_plot)]), 'rv', 'MarkerFaceColor', 'r');
% title(['Data with Detected Peaks for Column ' num2str(col_to_plot)]);
% xlabel('Time (s)');
% ylabel('Amplitude');
% grid on;
% Uncomment the following section to plot specific column troughs
% time = (0:length(data_col)-1) / fs;
% col_to_plot = 19; % Change this to plot a different column
% figure;
% plot(time, cma_filtered(:, col_to_plot));
% hold on;
% plot(peak_locations.(['col' num2str(col_to_plot)]) / fs,
peak_amplitudes.(['col' num2str(col_to_plot)]), 'rv', 'MarkerFaceColor', 'r');
% title(['Data with Detected Peaks for Column ' num2str(col_to_plot)]);
% xlabel('Time (s)');
% ylabel('Amplitude');
% grid on;
% %Extract stimulus timings from the hb data set and place in a matrix
%
% for stim_times = zeros(4,length(hb)); i=1:length(hb)
% temp = hb(i).stimulus.values{1,1}.onset;
% stim_times(:,i) = temp;
% clear temp
% end
% Extract pulse related data (height, slope, from each Stim (25 beats prior to
40 beats
% afterwards)
r_values = (0.1:0.01*std(peak_prominence.col3):0.25*std(peak_prominence.col3));
% to obtain a range of relevant r's to use in the sample entropy
% Calculate SampEn of the segment with a r= 0.15 *sd and a tolerance of m=2
saen2 = total_sample_entropy(peak_prominence.col3,2,r_values);
avgsampentropy = saen2/(length(r_values));

```